Conductivity studies for an electron surface layer on $Hg_{1-x}Cd_xTe$

Wen-qin Zhao* and F. Koch
Physik-Department, Technische Universität München, D-8046 Garching, Federal Republic of Germany

J. Ziegler and H. Maier
Telefunken Electronic, D-7100 Heilbronn, Federal Republic of Germany

(Received 30 July 1984)

We examine the electronic transport properties of the interfacial charge layer in a metal-oxide—semiconductor structure on $Hg_{1-x}Cd_xTe$. We focus, in particular, on the conductivity discontinuities incurred when different quantized levels of the surface layer are successively filled with rising carrier density N_s. Three types of levels are considered: the electric subbands, Landau levels in a perpendicular magnetic field ($B_\perp$), and the magnetoelectric (hybrid) levels for a magnetic field parallel to surface ($B_\parallel$).

I. INTRODUCTION

Interfacial charge at a semiconductor-insulator boundary is usually confined on a scale of length such that quantum effects are important. The confinement normal to the interface in the electrostatic potential gives rise to electric subbands $E_n+\hbar^2k_\parallel^2/2m^*$ with $n=0,1,2,\ldots$. In a field $B_\perp$, the bounded lateral motion in the form of cyclotron orbits causes additional quantization in terms of Landau levels $l=0,1,2,\ldots$. Each of the levels $E_n+(l+\frac{1}{2})\hbar\omega_c$ occurs as a plus or minus ($\pm$) spin-split pair. Finally, electric subbands in the presence of a strong $B_\parallel$ field are modified to become a qualitatively new type of level. These are the magnetoelectric (hybrid) subbands that have received attention in experimental studies of InAs (Ref. 1) and InSb (Refs. 2 and 3).

In this paper we consider the surface conductivity of the narrow-gap semiconductor $Hg_{1-x}Cd_xTe$. The experiments are intended to explore structures in the conductivity that occur with the filling of the three types of quantum levels—the electric subbands, the Landau levels, and the magnetoelectric bands. The successive filling of the levels is achieved in an N_s sweep of the gated metal-oxide—semiconductor (MOS) structure.

The semiconductor $Hg_{1-x}Cd_xTe$, together with its anodic oxide, is a system ideally suited for such experiments because of the high mobility of the interface carriers and easy access to the relevant range of experimental parameters. This is particularly true for the $B_\perp$ and $B_\parallel$ fields, where nearly any laboratory magnetic field is a high field. The magnetic splitting $\hbar\omega_c$ can easily exceed the electric energies in the problem. Moreover, the small two-dimensional (2D) density of states leads to a filling of several of the electric bands for modest values of the total charge density N_s.

The principle that structure in the density of quantized states is reflected in conductivity variations is thoroughly familiar from the large body of work on the Shubnikov—de Haas effect in 2D systems. The magnetic-field-induced conductivity structures are an integral part of the 2D electron-gas studies. Less well known and not always easily observed is the conductivity structure caused by successive filling of the electric bands. For this reason we show, in Fig. 1, an example from earlier work on InSb.[4] The conductivity derivative $d\sigma/dV_g$ has distinct structures at voltages $V_0,V_1,V_2,\ldots$ which correspond to surface-carrier-density values where the Fermi energy just coincides with the step in the density of states. The steps V_n have independently been confirmed from subband-occupancy studies with the Shubnikov—de Haas effect. Compared with the strong modulation of the conductivity familiar from the magnetoconductance experiments, the electric structures are weak and difficult to resolve experimentally. The reason for this is evident. There is only a small step in the density of states. Moreover, a change in the conductivity with increasing N_s requires that the scattering mechanisms be sensitive to the step in the density of states. The effect demonstrated in Fig. 1 is related to the discussion in Secs. III and V.

In Sec. II we have collected the experimental details regarding sample-preparation and measuring techniques. In Secs. III, IV, and V we deal with the three types of conductivity structures as caused by the electric, magnetic, and magnetoelectric quantized bands, respectively. We conclude with a summary and some final remarks in Sec. VI.

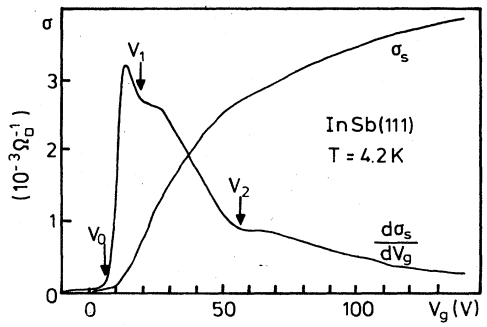

FIG. 1. Surface conductivity $\sigma_s(V_g)$ and its derivative for InSb. Structures in $d\sigma_s/dV_g$ at $V_0,V_1,V_2,\ldots$ signify the occupancy onset of electric subbands $n=0,1,2,\ldots$ ($1\ \mathrm{V}\approx 6.4\times10^9\ \mathrm{cm}^{-2}$) (after Ref. 4).

II. EXPERIMENTAL NOTES

$Hg_{1-x}Cd_xTe$ with $x \sim 0.2$ is a commonly used infrared photoconductive detector material. The high-quality oxide-semiconductor interfaces, as employed in the experiments here, are made by anodic oxidation. Such surface passivation is an essential step in detector technology. The surface treatment makes the interface electronically passive in that it removes traps, defect structures, irregularities, and unsaturated chemical bonds that can act as recombination centers. It provides a good interface for the gate-controlled MOS structures in the experiments.

The detector samples are in the form of strips 4×1 mm^2 in size and 10 μm thick. The insulator consists of ~ 0.1 μm anodic oxide and ~ 1 μm or ZnS coating. The metal gate is a Ni-Cr layer measuring 3×0.8 mm^2. Ohmic contacts are attached at the two ends of the n-type sample. The surface conductivity of this MOSFET-like structure (FET denotes field-effect transistor) is registered as additional conduction in a surface path. The bulk and surface-layer conductivities are comparable for the detector samples with a volume carrier density of $n \sim 10^{15}$ cm^{-3}.

In addition to the detectors with anodically oxidized surfaces, we make use of samples prepared with "natural" surfaces. Single-crystal slabs with thicknesses of ~ 400 μm are etched and dip-polished in a standard bromine-methanol solution. They are subsequently coated with an insulating lacquer in a commercial spinner. Such samples have flat-band conditions near zero gate voltage. Because of the greater thickness, the surface conduction amounts to usually only a few percent of the total conductivity.

The measurement procedures and apparatus are standard. Magnetic fields up to 8 T at 4.2 K are employed. The measuring currents are kept sufficiently small to assure negligible heating.

III. ELECTRIC SUBBANDS AND THE SURFACE CONDUCTIVITY

The surface-channel conductivity of the $Hg_{1-x}Cd_xTe$ detector samples is registered as a relative change in the total resistance. Typical for such data is the curve in Fig. 2 taken at 77 K. For this sample the surface channel starts to conduct at $V_g \sim -22$ V. The resistance continues to decrease with rising V_g and N_s. The value of the

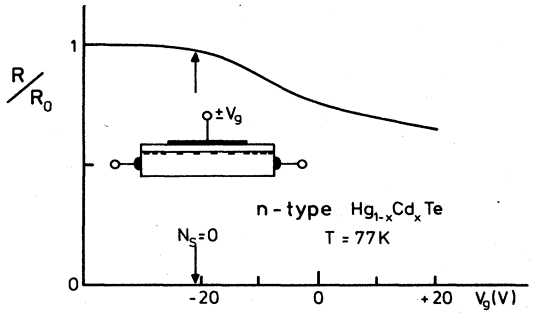

FIG. 2. Resistance variation of a detector sample with applied gate voltage V_g (1 V $\approx 5.5 \times 10^{10}$ cm^{-2}). The exact distribution of surface and bulk currents is not known. $N_s = 0$ occurs at -22 V.

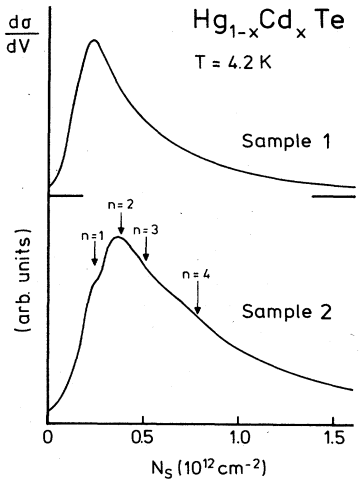

FIG. 3. Comparison of the field-effect mobilities of two detector samples. Points marked $n = 1$, 2, 3, and 4 indicate the onset of occupancy of the corresponding subband.

resistance change is such that, for $N_s \sim 1 \times 10^{12}$ cm^{-2}, a surface mobility $\sim 60\,000$ cm^2/V sec applies. Because of the unknown distribution of current flow in the sample, the estimated mobility could be in error by as much as a factor of 2. After repeated cycles of electrical stress at negative V_g, a gradual shift of the onset voltage to more negative values is found.

In order to search for subband-quantization effects, analogous to those for InSb (Fig. 1), it is necessary to examine the derivative $d\sigma/dV_g$. We have done so in a number of detector samples and have seen distinct structure in $d\sigma/dV_g$ for some of them. Data are shown in Fig. 3 for the pair of samples for which much of the following data has been taken. Of these, $d\sigma/dV_g$ structures indicating occupancy of a new subband are found only in the lower of the two curves. The overall shape of the two curves is quite different, suggesting different relative contributions of charged-impurity and surface-roughness scattering. The small amplitude of the $d\sigma/dV_g$ structures results from the small discontinuities in the density of states and the insensitivity of the conductivity to this density of states. Fluctuations in the interface potential would also act to smear out the subband onset. The point to be made here, however, is that under appropriate conditions the occupancy onsets of the electric surface bands can be observed.

IV. LANDAU LEVELS: CONDUCTIVITY OSCILLATIONS IN A $B_\perp$ FIELD

The application of a magnetic field perpendicular to the surface leads to the well-known Landau quantization. A ladder of levels $l = 0,1,2,\ldots$ exists for every one of the electric subbands. Because of the high mobility of the interface carriers in the detector samples, magneto-oscillations of the conductivity are already observed at modest values of $B_\perp$. There have been several reports of the effect for $Hg_{1-x}Cd_xTe$ in the literature.[5-7]

The primary objective of the $B_\perp$ experiments is to iden-

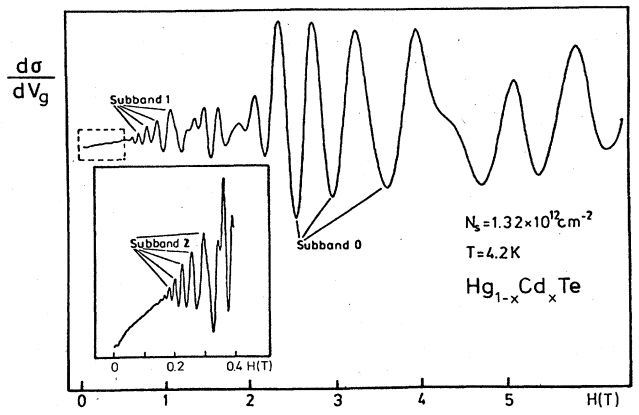

FIG. 4. Conductivity derivative oscillations in a perpendicular magnetic field. Contributions from subbands 0, 1, and 2 are identified. The density $N_s = 1.32 \times 10^{12}$ cm^{-2} corresponds to $V_g = 0$ V in this sample and represents natural accumulation.

tify occupied subbands and measure their occupancies from the period of the conductivity oscillations. Care must be taken to avoid high values of $B_\perp$ at low N_s where a field-induced redistribution of carriers between the subbands must occur. This situation is easily achieved in $Hg_{1-x}Cd_xTe$ where the Landau-level or spin splitting can exceed the subband energies.

Shubnikov—de Haas data from all detector samples with $x \sim 0.2$ were practically identical. Possible errors, small discrepancies, or differences in the oscillation spectrum could be traced to uncertainties in the threshold determination or errors in the capacitance needed to convert the gate voltage to an N_s value. When several subbands are occupied, it is best to take data in a $B_\perp$ sweep at fixed N_s. Figure 4 is an example for a detector sample with $x \simeq 0.20$. The inset shows that oscillations persist to 0.15 T.

In evaluating the oscillation periods, we identify three partly filled surface bands. The collection of data points in Fig. 5 applies for several detector samples with bulk x values ranging between 0.19 and 0.21. Because experimental results on subband spectroscopy,[8] cyclotron resonance, and photoresponse measurements[9] on detector samples pointed to a reduce E_g in the surface layer, we have

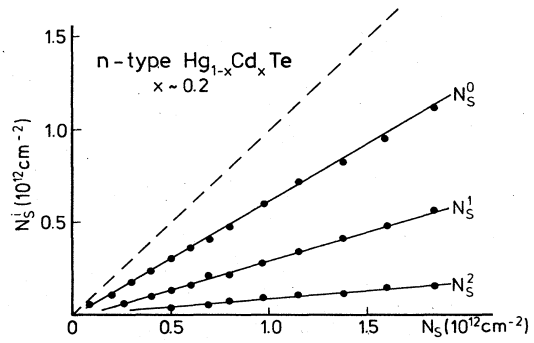

FIG. 5. Partial occupancies of the first three subbands vs N_s for accumulation layers on samples with $x \simeq 0.2$.

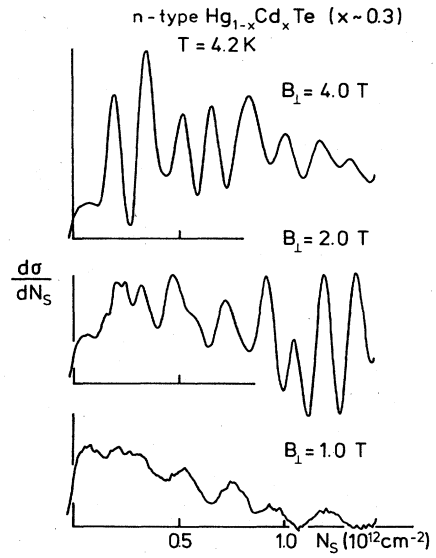

FIG. 6. Magnetoquantum oscillations vs N_s for a lacquer-covered sample with $x \simeq 0.3$.

carefully compared Shubnikov—de Haas data from the anodically oxidized detector and "naked-surface"-type samples. Data from the latter are not as good. The surface mobility is lower and fields above 0.6 T are necessary to observe oscillations. Because of the field-dependent bulk conductivity of the thick samples it is preferable to make N_s-sweep measurements. Within experimental error, the two types of samples for x in the 0.2 range give the same result. We can state succinctly that, for accumulation layers and $N_s \geq 1 \times 10^{12}$ cm^{-2}, partial occupancies are $0.62N_s$, $0.27N_s$, and $0.08N_s$ for the first three subbands. The estimated uncertainty in each of these numbers is ± 0.02. The occupancy onsets are consistent with those marked on Fig. 3. For accumulation, it is necessary to recall that onset occurs with a jump in N_s^n.[10]

We have also studied the Shubnikov—de Haas effect in samples for which $x \sim 0.3$. These were lacquer-covered specimens with thicknesses of ~ 0.4 mm. Data were obtained in V_g sweeps at constant $B_\perp$. The flat-band voltage V_{FB} occurs near $V_g = 0$ V. The type of data that could be obtained on such "homemade" specimens is shown in Fig. 6. The maximal N_s achieved on these samples is only 1.5×10^{12} cm^{-2}. The fractional occupancies of three subbands have been identified and can be expressed as $0.70N_s$, $0.23N_s$, and $0.07N_s$, with an estimated error of $\pm 0.02N_s$. The occupancy of the 0 subband is relatively greater than that in $x \simeq 0.2$ specimens, and those of higher subbands are less. This is consistent with what is expected for a material with larger E_g. The numbers agree with those of Ref. 7.

V. MAGNETOELECTRIC SURFACE BANDS: CONDUCTIVITY STRUCTURES IN A $B_{||}$ FIELD

It is known that the energies of the electric surface bands are shifted in a $B_{||}$ field. In the limit of small $B_{||}$, the effect can be described in perturbation theory. The diamagnetic energy shift is proportional to $B_{||}^2$. Small

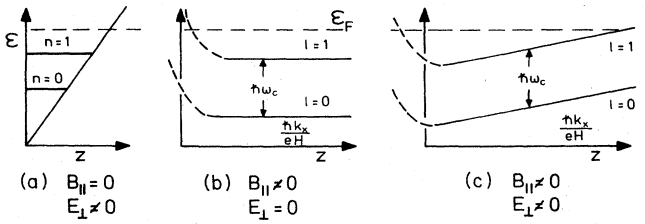

FIG. 7. Surface bands for various configurations of $E_\perp$ and $B_{||}$. Panel (c) is a description of the magnetoelectric levels, assuming the magnetic energy to be the dominant source of contributions. The electric field $E_\perp$ is taken to be constant ignoring self-consistency of the potential.

fields are such that the corresponding cyclotron radius is much greater than the binding length of the particular subband. For the nonparabolic surface bands of $Hg_{1-x}Cd_xTe$, the effect of $B_{||}$, even in this weak-field limit, has not been worked out. It is clear from the experiments that weak $B_{||}$ means fields of much less than 1 T.

For typical (1–10)-T laboratory fields, the magnetic energy $\hbar\omega_c$ dominates the characteristic subband binding energy. For example, $\hbar\omega_c \sim 30$ meV for $B_{||}=2.4$ T. The largest energy separation E_{01} in a detector sample at $N_s=1\times10^{12}$ cm^{-2} is ~ 18 meV. Other E_{nm} are much less. We argue that the effect of $B_{||}$ for $Hg_{1-x}Cd_xTe$ should be considered in terms of the high-$B_{||}$ limit. The evolution of the electric surface bands $n=0,1,\ldots$ into magnetoelectric levels can be followed in the schematic diagram of Fig. 7. The pure Landau levels $l=0,1,\ldots,$ with the exception of orbits intersecting the surface at $z=0$, are independent of the position of the orbit center in the sample. In Fig. 7(c) these are changed by the addition of an electric energy $eE_\perp\langle z\rangle$. Here, $\langle z\rangle$ is the orbit-center location in the sample, and the field is taken to be uniform in the sample. Nonparabolicity and self-consistency of the electrostatic potential are neglected in the construction of Fig. 7(c). The occupancy of the magnetoelectric bands includes a one-dimensional sum over the k_y states ($B_{||}$ is along $\hat{y}$) up to the Fermi energy. In this sense the problem resembles the usual Landau-level situation.

The effect on the conductivity of filling successive magnetoelectric bands in an N_s sweep at fixed $B_{||}$ resembles the situation discussed in Sec. III. In terms of Fig. 7(c), the energy E_F rises and touches the next-higher magnetoelectric band. With the filling of the surface layer the electric field $E_\perp$, and with it the slope of the energy versus z, also rises. The conductivity structures indicate the onset of occupancy of the next-higher magnetoelectric band. This is, in essence, the model proposed in Refs. 1 and 11.

Conductivity structures caused by the magnetoelectric bands are shown in the data of Fig. 8. The curves are for a detector-type sample with $x=0.20$. The $d\sigma/dV_g$ minima shift with increasing $B_{||}$ to higher N_s. All but the first minimum, labeled 0^+, appear as doublet pairs. We suggest that this represents spin splitting and assign numbers 1^-, 1^+, 2^-, 2^+, etc. to denote spin-split, magnetoelectric bands that are successively filled with rising N_s.

The evaluation of Fig. 8 yields straight-line plots relating the N_s position of a given minimum to $B_{||}$. For fields above 1 T, the points in Fig. 9 lie on perfectly straight lines. 0^+ appears as a single line. The 0^- band fills at $N_s=0$ and is a vertical line in this plot. There is presently no satisfactory explanation why, in spite of nonparabolicity, self-consistency screening in the surface potential, and the surface perturbations on the magnetoelectric bands [Fig. 7(c)], there should be a linear relation of $B_{||}$ and N_s. This is a fascinating aspect of this work that deserves further attention.

The spin-splitting energy for $Hg_{1-x}Cd_xTe$ is known and provides, in principle, a way to convert the $B_{||}$ axis into an energy scale. Resonance experiments give a spin energy of ~ 23 meV at 5 T for $x\simeq 0.2$ material in the

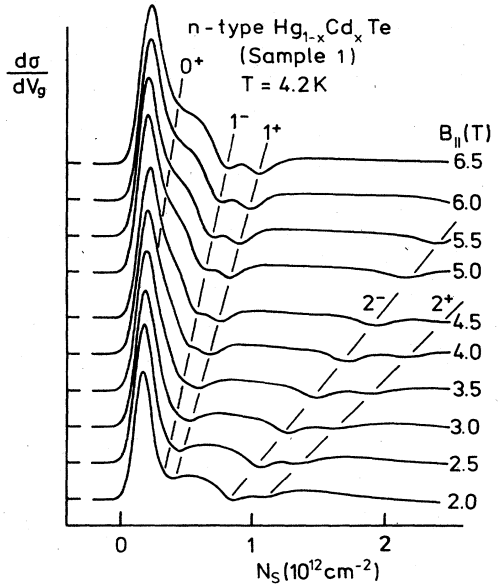

FIG. 8. Conductivity derivative in a magnetic field parallel to the surface. The structures as marked give the onset of filling for the spin-split pairs of magnetoelectric bands.

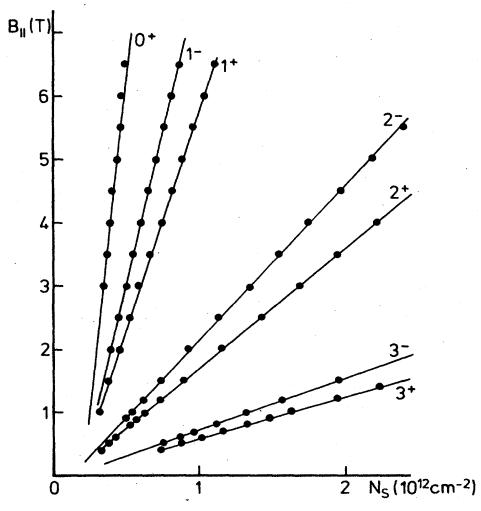

FIG. 9. $B_{||}$-vs-N_s relation for the conductivity structures caused by the magnetoelectric bands $l^\pm$.

$l=0$ Landau level.[12] Because of nonparabolicity, the splitting decreases in the case of $l=1,2,\ldots$. It has not been measured in these levels. Because of the uncertainty regarding the x value in the surface layer,[9] assignment of absolute energy values to Fig. 9 cannot be justified at present. We note that the splitting $\Delta B_{||}$ of the l^-,l^+ pairs in Fig. 9 about some fixed $B_{||}$ are nearly the same. Moreover, at fixed N_s the ratio of $\Delta B_{||}$ to the average $B_{||}$ corresponds closely to the known ratio of spin and cyclotron energies. It is of interest in this regard to note that in $B_{||}$ cyclotron resonance the m_c^* in the surface layer is measured as the value of the $l=0$ to $l=1$ transition for all N_s.[13]

To show that the simple description of the magnetoelectric bands in Fig. 7(c) gives a reasonable quantitative account of the data in Fig. 9, we carry out a simple calculation. We integrate over k_y and sum over orbit centers (i.e., k_x) in order to arrive at an expression for the $l=1^{\pm}$ minimum. For this, the energy E_F must lie $\hbar\omega_c$ above the $l=0$ energy at $z=0$. One arrives at the relation

$$N_s=\frac{4\sqrt{2}}{3\pi^2}\frac{B_{||}^{5/2}}{\hbar^{1/2}E_{\perp}m^*}\ .$$

The field $E_{\perp}$ is in some way linked with N_s. Because of screening, $E_{\perp}$ is not constant as the model assumes. It is reasonable to take it to be one-half of the value at $z=0$, i.e.,

$$E_{\perp}=\frac{1}{2}\frac{N_s e}{\epsilon}$$

which for $N_s=1\times10^{12}$ cm^{-2} and $\epsilon=13$ gives 0.7×10^5 V/cm. With the measured $m_c^*=0.007m_0$, the $B_{||}$ necessary to achieve the cutoff condition for $l=1$ is estimated to be ~12 T. The measured value from Fig. 9 is 7 T. In view of the many approximations, this is a surprisingly good estimate. One can go a step further and calculate the depth to which the charge extends, as $z_{\max}=\hbar\omega_c/eE_{\perp}\approx300$ Å. We conclude that the simple model gives reasonable magnitudes. The relation of $B_{||}$ to N_s results in $B_{||}\propto N_s^{0.8}$, instead of the experimentally determined linear relation. As a further point, we note that the ratios of slopes of the $l=1$, 2, and 3 lines in Fig. 9 resemble the partial occupancy plots from the Shubnikov–de Haas studies in Fig. 5. The same is true for data given in Ref. 1.

It remains to consider the case for small $B_{||}$, i.e., how the weak structures in Fig. 3 evolve into the distinct spin-split minima in Fig. 8. For $B_{||}=0$ the $d\sigma/dV_g$ structures lie at finite N_s, and for sufficiently weak fields, such that a perturbation description applies, they must shift as $B_{||}^2$. It is clear that with the application of $B_{||}$ the amplitude of the structure grows. This is evidence for the evolution of the discontinuity in the density of states in a magnetic field $B_{||}$. It is possible to trace back a given structure with decreasing $B_{||}$ and show that the variation $B_{||}$ versus N_s is not linear. Nevertheless, the amplitude vanishes so quickly that the marking procedure is not very accurate.

VI. SUMMARY: A COMPARISON WITH InSb AND InAs

We have considered various types of quantum levels in an interfacial charge layer on $Hg_{1-x}Cd_xTe$, and have examined the structures that occur in the conductivity with the filling of such levels. For the electric subbands and $B_{\perp}$ Landau levels, we have been able to relate the effects to well-known models. From Shubnikov–de Haas effect data we have determined the partial occupancies of the first three subbands for samples with $x\simeq0.2$ and 0.3.

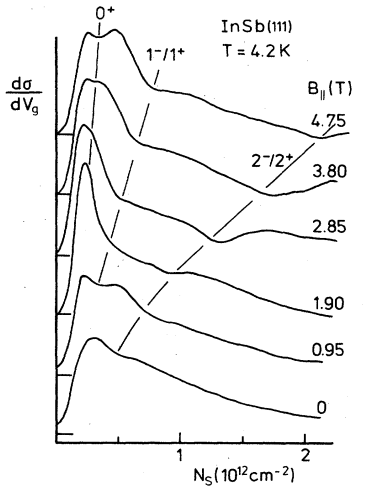

FIG. 10. Parallel field magnetoconductivity vs N_s for InSb (after Ref. 11).

For the discussion of the effects of a $B_{||}$ field there does not exist an exact description, so we have relied on the qualitative ideas that have evolved from previous work on InSb and InAs. The basic idea of an onset of occupancy of a next-higher subband suggests itself naturally from the effect for $B_{||}=0$. In this paper we have derived a simple expression based on a high-$B_{||}$ limit that allows a quantitative evaluation of the parameters and gives, approximately, the linear $B_{||}$-versus-N_s dependence which is observed experimentally.

Despite these partial successes, the model is not adequate. The fact that in the presence of strong nonparabolicity and screening effects in the surface potential one still observes a strictly linear $B_{||}$ versus N_s suggests a more fundamental relation between the various physical parameters than that derived in Sec. V. It is this thought that has prompted us to compare the $B_{||}$-conductivity spectra of the three materials InSb, InAs, and

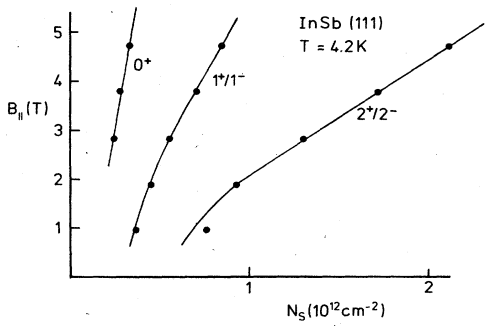

FIG. 11. $B_{||}$-vs-N_s relation for the conductivity structures observed on InSb. Note the curvature at low $B_{||}$.

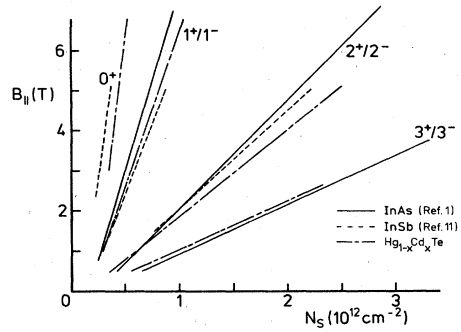

FIG. 12. Comparison of the $B_{||}$-vs-N_s data for three different materials. The InAs data are from Ref. 1; the InSb data is from Ref. 11.

$Hg_{1-x}Cd_xTe$. Contrasting the present Fig. 9 to data in Ref. 1 on InAs, it is clear that the m^* dependence of the model is not satisfied. The latter requires the slope of $B_{||}$ versus $N_s^{0.8}$ to scale with $m^{*1/2}$.

We show in Fig. 10 data from InSb (111). The insulator is a 6-μm-thick Mylar foil, and the measured capacitance gives a carrier density of 3.0×10^9 cm^{-2}V^{-1}. The structures are not as distinct as those in Fig. 8; the spin splitting cannot be identified, but there is some resemblance. The $B_{||}$-versus-N_s plots in Fig. 11 stress this similarity in assigning the labels 0^+, $1^\pm$, and $2^\pm$ to the lines. The latter two represent the unresolved average value of the spin pairs of the magnetoelectric bands. The spin-splitting for InSb is sufficiently large for a splitting of the $l=0$ bands to be expected. The surprise contained in this manner of assignment is that the straight-line plots of Figs. 9 and 11 are the same within reasonable experimental uncertainty. Moreover, the InAs data of Ref. 1 will also fit the scheme. We recall that the g factor of InAs is -15. For InSb ($g=+127$) and $Hg_{1-x}Cd_xTe$ ($g=-164$) the spin splittings are nearly an order of magnitude greater. Thus it is unlikely that 0^+ will be observable for InAs. Using the same labeling as in this paper, the $i=0$ line of Ref. 1 is $1^\pm$, while $i=1$, 2, and 3 correlate with $2^\pm$, $3^\pm$, and $4^\pm$, respectively. The lines plotted in Ref. 1 for InAs then are identical with those for InSb and $Hg_{1-x}Cd_xTe$. Figure 12 gives the comparison of the straight-line plots for the three materials.

We do not really want to suggest that the $B_{||}$-versus-N_s straight-line plots for the magnetoelectric bands of all surface charge layers are universal. It is easy to see that this cannot be true by considering the inversion case with arbitrary depletion charge N_{dep}. The onset points can be moved to arbitrarily high N_s by just raising N_{dep}. Such a situation, because of the strong electric binding, will then not represent a limiting high-$B_{||}$ case. The three cases discussed here apply to accumulation or inversion with small N_{dep}. The fractional occupancy N_s^n-versus-N_s plots are nearly the same for all three.

It is speculation, but the thought of linking the occupancies N_s^n with the $B_{||}$-versus-N_s plots suggests itself. At given $B_{||}$ there occur several structures at various N_s values (compare Fig. 8). Weighting these according to the fractional occupancy for the assigned level, one arrives at a number of electrons that is within $\pm20\%$ of 1×10^{11} cm^{-2}T^{-1} for a spin-degenerate magnetoelectric band when the onset of the next-higher band occurs. The rule holds within reasonable experimental uncertainties for all three semiconductors studied so far. One is reminded of a degeneracy factor such as that occurring for $B_\perp$ in two dimensions ($\sim0.5\times10^{11}$ cm^{-2}T^{-1}). A degeneracy factor argument for the $B_{||}$ data has the attractive feature of giving a linear $B_{||}$-versus-N_s relation, as well as being independent of m^* and the exact form of the electrostatic potential. At present, however, we conclude that further thought and more extensive experimental work on other substances is required.

*Permanent address: Shanghai Institute of Technical Physics, Academia Sinica, Shanghai, People's Republic of China.

[1]R. E. Doezema, M. Nealon, and S. Whitmore, Phys. Rev. Lett. **45**, 1593 (1980).

[2]F. Koch, in *Physics in High Magnetic Fields,* Vol. 24 of *Springer Series in Solid-State Sciences,* edited by S. Chikazumi and N. Miura (Springer, Berlin, 1981), pp. 262—273.

[3]J. H. Crasemann, U. Merkt, and J. P. Kotthaus, Phys. Rev. B **28**, 2271 (1983).

[4]A. Därr, doctoral dissertation, Technische Universität München, 1977.

[5]G. A. Antcliffe, R. T. Bate, and R. A. Reynolds, in Proceedings of the Conference on the Physics of Semimetals and Narrow-Gap Semiconductors, Dallas (1970) [J. Phys. Chem. Solids **32**, Suppl. 1, 499 (1971)].

[6]S. Narita, T. Kuroda, Y. Nisida, in *Proceedings of the 14th International Conference on Physics of Semiconductors,* Edinburgh, 1978, edited by B. L. H. Wilson (IOP, London, 1979), p. 1235.

[7]J. P. Dufour, R. Machet, J. P. Viton, J. C. Thuillier, F. Baznet, in *Insulating Films on Semiconductors,* Vol. 7 of *Springer Series in Electrophysics,* edited by M. Schulz and J. Pensl (Springer, Berlin, 1981), p. 259.

[8]J. Scholz, F. Koch, J. Ziegler, and H. Maier, Surf. Sci. **142**, 447 (1984).

[9]J. Scholz, E. Schindlbeck, F. Koch, H. Maier, and J. Ziegler, US Workshop on the Physics and Chemistry of $Hg_{1-x}Cd_xTe$, San Diego, 1984 (unpublished).

[10]H. Reisinger, H. Schaber, and R. E. Doezema, Phys. Rev. B **24**, 5960 (1981).

[11]H. Grassl, diploma thesis, Technische Universität München, 1975 (unpublished).

[12]E. Schindlbeck, diploma thesis, Technische Universität München, 1983; F. Koch, in *Two-Dimensional Systems, Heterostructures and Superlattices,* Vol. 53 of *Springer Series in Solid-State Sciences,* edited by G. Bauer, F. Kuchar, and H. Heinrich (Springer, Berlin, 1984) pp. 20—31.

[13]Wen-qin Zhao, C. Mazuré, F. Koch, J. Ziegler, and H. Maier, Surf. Sci. **142**, 400 (1984).